J BONE ONCOL 35 (2022) 100436

Contents lists available at ScienceDirect

Journal of Bone Oncology

journal homepage: www.elsevier.com/locate/jbo

Research Paper

Circ_0051079 silencing inhibits the malignant phenotypes of osteosarcoma cells by the TRIM66/Wnt/β-catenin pathway in a miR-625-5p-dependent manner

Weilin Wang, Jianhua Wang, Yingyi Li, Yongxu Zhao *

Department 2 of Orthopedics, The Fifth people's Hospital Of Dalian, NO. 890 Huanghe Street, Shahekou District, Dalian, Liaoning, China

ARTICLE INFO

Keywords:
OS
Circ_0051079
miR-625-5p
TRIM66
Wnt/β-catenin pathway

ABSTRACT

Background: Circular RNA (circRNA) is a newly-discovered endogenous transcript that has been reported to participate in osteosarcoma (OS) progression. However, the underlying mechanism of circ_0051079 modulating OS development remains unclear.

Methods: RNA expressions of circ_0051079, miR-625-5p and tripartite motif containing 66 (TRIM66) were detected by quantitative real-time polymerase chain reaction. Protein expression was checked by Western blot analysis. The functional effects of circ_0051079 on OS cell malignancy were investigated by cell counting kit-8, clonogenicity, transwell, tube formation and flow cytometry assays. The interactions among circ_0051079, miR-625-5p and TRIM66 were identified by dual-luciferase reporter and RNA immunoprecipitation assays. Mouse xenograft model assay was performed to elucidate the effects of circ_0051079 knockdown on tumor formation *in vivo*.

Results: Circ_0051079 and TRIM66 expressions were significantly upregulated, but miR-625-5p was down-regulated in OS tissues and cells compared with control groups. Circ_0051079 expression was significantly associated with tumor-node-metastasis stage and tumor size of OS patients. Circ_0051079 knockdown inhibited OS cell proliferation, migration and invasion, repressed angiogenesis but induced cell apoptosis, accompanied by the decreases of PCNA and Bcl-2 production and an increase of Bax production. MiR-625-5p, a target miRNA of circ_0051079, participated in regulating circ_0051079-induced effects. Also, TRIM66 was identified as a target mRNA of miR-625-5p, and partially attenuated the inhibitory effects of miR-625-5p in OS cells. Circ_0051079 modulated the Wnt/β-catenin pathway through TRIM66 *in vitro*. Importantly, circ_0051079 silencing reduced TRIM66 expression by interacting with miR-625-5p. Further, circ_0051079 depletion inhibited tumor formation *in vivo*.

Conclusion: Circ_0051079 regulated OS development by the miR-625-5p/TRIM66/Wnt/β-catenin pathway, providing a novel therapeutic target for OS.

1. Introduction

Arising from malignant mesenchymal cells, osteosarcoma (OS) is a lethal primary bone cancer that is common in children and teenagers [1]. Fast proliferation and high metastatic properties are considered as the main reason for the poor clinical outcome of OS patients [2]. Osteosarcoma cases can benefit from medical therapies like small molecular targeting treatment, surgery, chemotherapy and radiotherapy, but these strategies often fail in clinical trials [3,4]. Consequently, more practical researches and investigations on the molecular mechanism of OS development are necessary to discover specific therapeutic targets for OS.

Recently, studies on circular RNA (circRNA) have become a burgeoning topic related to cancer development. As a newly-found endogenous noncoding RNA, circRNA forms a covalently closed continuous loop by a back-splicing event [5]. The cyclic structure can protect circRNA from digestion by exonuclease [6]. An increasing number of researches have suggested that circRNA is dysregulated in different types of cancers, and these circRNAs have the potential as diagnostic or therapeutic markers, such as circ_0058124 [7], circ_100395 [8] and circ_0014130 [9]. CircRNA regulates the biological behaviors of cancer cells mainly by sponging microRNA (miRNA), interacting with RNA

* Corresponding author.
E-mail address: zhaoyongxu119@163.com (Y. Zhao).

https://doi.org/10.1016/j.jbo.2022.100436
Received 16 January 2022; Received in revised form 31 May 2022; Accepted 1 June 2022
Available online 2 June 2022

binding protein or acting as protein scaffolds [10]. Substantial evidence has shown that circRNA is involved in OS cell proliferation, invasiveness and metastasis [11]. Circ_0051079 is located in chr19:40747844-40771258, and is one of the 15 most increased circRNAs in OS tissues [12]; however, its function and mechanism in OS has not been systematically investigated.

As small single-stranded molecules, miRNAs are featured by high stability and conservation. MiRNAs are a class of posttranscriptional regulatory molecules that can bind to mRNA, leading to mRNA degradation and translation repression [13]. MiRNA abnormality can be found in multiple cancers like colorectal adenocarcinoma, renal cancer, acute myeloid leukemia and OS [14,15]. MiR-625-5p commonly acts as a cancer-suppressing molecule, and previous data have indicated its importance in lung cancer [16], cervical cancer [17] and glioma [18]. However, how miR-625-5p acts function in OS development still needs further investigation.

Tripartite motif containing 66 (TRIM66) is a tripartite motif (TRIM)-containing protein and is defined by the presence of PHD and BROMO domains [19,20]. It has been well accepted that the protein negatively regulates postmeiotic genes through association with recombinant chromobox homolog 3 (CBX3) and centromeres. Besides, a considerable report suggested that TRIM66 was required for transformation potential of cancer cells by modulating GSK-3β-dependent Wnt/β-catenin signaling [21]. According to the competing endogenous RNA hypothesis that indicated that circRNA acts as a rival to mRNA by combining with miRNA [22], we predicted the relationships among circ_0051079, miR-625-5p and TRIM66 through circular RNA interactome (https://circinteractome.nia.nih.gov/index.html) and targetscan (https://www.targetscan.org/vert_71/) databases. As a result, miR-625-5p potentially bound to circ_0051079 and TRIM66. However, whether circ_0051079 mediates OS development by the miR-625-5p/TRIM66 pathway remains far from being addressed.

Herein, we analyzed the relative expression of circ_0051079, explored its potential functions in OS cell malignancy and determined whether the circ_0051079/miR-625-5p/TRIM66 pathway was responsible for OS malignant progression.

2. Materials and methods

2.1. Study subjects

A total of 55 OS patients in the Fifth people's Hospital of Dalian were enrolled in the present study with approval from the Ethics Committee of the Fifth people's Hospital of Dalian. Fifty-five OS tissues were divided into 23 stage I-II OS tissues, 32 stage III OS tissues, 25 OS tissues sized $<$ 5 cm and 30 OS tissues sized $>$ 5 cm. The neighboring noncancerous specimens were collected 5 cm from the tumor margin. All samples were immediately stored at −80 °C. The participants signed the written informed consent prior to receiving surgery.

2.2. Cell culture

Human normal fetal osteoblast (hFOB1.19), OS cell lines (U2OS, HOS and SaoS2) and human umbilical vein endothelial cells (HUVECs) were purchased from Procell (Wuhan, China), and cultured in Dulbecco's modified Eagle's medium (DMEM; Weike Biotechnology, Shanghai, China), McCoy's 5a medium (Gibco, Carlsbad, CA, USA) or Ham's F12K (Procell) added with fetal bovine serum (FBS; Biosun, Shanghai, China) and 1% penicillin/streptomycin (Gibco). hFOB1.19 cells were cultured at 34 °C, and other cells grew at 37 °C.

2.3. Quantitative real-time polymerase chain reaction (qRT-PCR) and RNA treatment

RNA extraction reagent (Corning, Madison, New York) was used to isolate RNA from tissues and cells. RNA quality was analyzed through agarose gel electrophoresis of RNA. Reverse transcription of RNA was performed using high-capacity cDNA synthesis kits (Thermo Fisher, Waltham, MA, USA) and Tsingke (Shanghai, China). Next, Fast qPCR Mix (Tsingke) was used to analyze gene expression on an ABI StepOne qRT-PCR Machine (Thermo Fisher). Gene expression was normalized to U6 and glyceraldehyde 3-phosphate dehydrogenase (GAPDH) by the $2^{-\Delta\Delta Ct}$ method. Two μg of RNA was utilized to incubate with 6 U RNase R (Xiyuan Biotech, Shanghai, China) to identify the stability of circ_0051079. The primer sequences are listed in Table 1.

2.4. Cell transfection

The small interfering RNAs of circ_0051079 (si-circ_0051079#1, 5′-AGTCATCATTGCCAAGACTGT-3′; si-circ_0051079#2 5′-ATTGCCAAGACTGTGCCCTGT-3′; si-circ_0051079#3 5′-TCATTGCCAAGACTGTGCCCT-3′), specific miR-625-5p mimics (miR-625-5p, 5′-AGGGGGAAAGUUCUAUAGUCC-3′) and inhibitors (anti-miR-625-5p, 5′-GGACUAUAGAACUUUCCCCCU-3′), and controls (si-NC, miR-NC and anti-miR-NC) were synthesized by GenePharma (Shanghai, China). The coding sequence of TRIM66 was synthesized and introduced into the pcDNA 3.1 vector (vector) to build the overexpression plasmid of TRIM66 (TRIM66). The lentiviral expressing small hairpin RNA of circ_0051079 (sh-circ_0051079) or sh-NC were packaged using polybrene (GenePharma). Then, cells growing in 24-well plates were transfected with 20 pmol siRNA, 0.8 μg plasmid, 100 nM miRNA mimics or 200 nM miRNA inhibitors using Polyplus-transfection® (Illkirch, France), referring to the standard methods.

2.5. Cell proliferation analysis

For cell counting kit-8 (CCK-8) assay, U2OS and SaoS2 cells were passaged in 32 mm petri dishes and transfected with test compounds, followed by culturing for 0, 1, 2 and 3 days, respectively. Then, CCK-8 kit (Dojindo, Shanghai, China) was used to analyze the samples following the instruction of manufacture. At last, the absorbance at 450 nm was measured using a microporous plate spectrophotometer (Bio-Tek, Winooski, VT, USA).

For clonogenicity assay, 2 mL McCoy's 5a medium (Gibco) containing 500 U2OS or SaoS2 cells was seeded into 6-well plates with three duplicate holes per group. After being transfected with plasmids or oligonucleotides, the cells were cultured for 10–14 days in an incubator. The cells were fixed with paraformaldehyde (Phygene, Fuzhou, China) and stained with crystal violet (Topscience; Shanghai, China). Finally, the colonies consisting of 50 or more cells were counted under an optical microscope.

2.6. Transwell assay to analyze cell migration and invasion

U2OS and SaoS2 cells at 55–75% confluence were employed for cell transfection. After 24 h, the cells were collected and seeded in the upper chambers of 24-well transwell chambers at a density of 5×10^4 cells per

Table 1
Primers sequences used for qRT-PCR.

Name		Sequences (5′-3′)
hsa_circ_0051079	Forward	TGGCAAAGTCATCCTGGTG
	Reverse	GCGTGGTACGCTGTCACCTA
AKT2	Forward	GCTAGGTGACAGCGTACCAC
	Reverse	GTCGCTCTTCAGCAGGAAGT
miR-625-5p	Forward	AGGGGGAAAGTTCTATAGTCCGC
TRIM66	Reverse	CTCTACAGCTATATTGCCAGCCAC
	Forward Reverse	CAGCAGGAAGAGGGGTCTTG
		GGTTCCAGGTAACCCAGCTC
GAPDH	Forward	CAAATTCCATGGCACCGTCA
	Reverse	GACTCCACGACGTACTCAGC
U6	Forward	CTTCGGCAGCACATATACT
	Reverse	AAAATATGGAACGCTTCACG

well, which were precoated with Matrigel (Corning) and added with FBS-free McCoy's 5a medium (Gibco). As a chemoattractant, the McCoy's 5a medium containing 15% FBS was added into the lower chambers. At 24 h after culture, the cells on the top surface of the lower chambers were stained using crystal violet (Topscience). Eventually, the invading cells from 5 high-power fields were observed under an inverted microscope (Olympus, Tokyo, Japan). Besides, the transwell chambers not coated with Matrigel were utilized to analyze cell migratory capacity according to the above method.

2.7. Capillary-like network formation

The tube formation assay was performed to investigate the angiogenesis of OS cells, referring to the reference [23]. 96-well plates were polymerized with growth factor-reduced Matrigel (Corning). In brief, HUVECs were cultured in 6-well plates for 48 h and digested using trypsin (Thermo Fisher), followed by diluting in U2OS and SaoS2 cell-conditioned medium. The cells were cultured in 96-well plates for 18 h, and the number of branch points was then analyzed using Image J software.

2.8. Flow cytometry analysis

The assay regarding Annexin V-FITC apoptosis detection kit (KeyGen, Nanjing, China) was performed to analyze cell apoptosis referring to the guidebook. In short, the transfected cells were harvested after 48 h of transfection and diluted using Binding Buffer, followed by incubation with Annexin V-FITC and propidium iodide in the dark. Finally, apoptotic cells were quantified with flow cytometer (Thermo Fisher).

2.9. Western blot analysis

With respect to the detection of protein expression, Western blot was carried out as previously described [24]. After 48 h of transfection, cells were harvested for analysis of protein expression. In brief, a total of 20 μg protein extract from tissues and cells was loaded onto polyacrylamide gels and transferred onto nitrocellulose membranes prior to blocking aspecific signals using defatted dry milk. Then, the membranes were incubated with the antibodies of proliferating cell nuclear antigen (PCNA; 1:1000; Thermo Fisher), B-cell lymphoma 2 (Bcl-2; 1:500; Thermo Fisher), Bcl-2-like protein 4 (Bax; 1:6000; Thermo Fisher), TRIM66 (1:1000; Thermo Fisher), β-catenin (1:2000; Affinity, Nanjing, China), c-myc (1:1000; Thermo Fisher), cyclinD1 (1:2000; Affinity), MMP2 (1:3000; Abcam, Cambridge, UK) and MMP9 (1:5000; Abcam) and GAPDH (1:400; Thermo Fisher). The blots were probed with secondary antibodies (1:4000; Thermo Fisher). At last, protein visualization was achieved using eyoECL Plus (Beyotime, Shanghai, China).

2.10. Dual-luciferase reporter assay

The putative associations among circ_0051079, miR-625-5p and TRIM66 were predicted through circular RNA interactome (https://circinteractome.nia.nih.gov/index.html) and targetscan (http://www.targetscan.org/vert_71/) databases. Circ_0051079 and TRIM66 3′UTR sequences containing the complementary sites of miR-625-5p were amplified and introduced into the pmirGLO vector to build wild-type plasmids (WT-circ_0051079 and WT-TRIM66 3′UTR). The binding sites of miR-625-5p within circ_0051079 and TRIM66 3′UTR were mutated by GenScript Biotech Corporation (Nanjing, China) to build mutants (MUT-circ_0051079 and MUT-TRIM66 3′UTR). Sequentially, the reporter plasmids were transfected into OS cells with miR-625-5p mimics or mimic control according to the above methods. Forty-eight-hour culture later, the cells were harvested for the analysis of luciferase activity with Dual-Lucy Assay Kit (Solarbio, Beijing, China).

2.11. RNA binding protein immunoprecipitation (RIP)

U2OS and SaoS2 cells were re-suspended in RIP lysis buffer (Millipore, Bradford, MA, USA) added with RNasin (TaKaRa, Dalian, China) and protease inhibitor (Roche, Basel, Switzerland). Then, the lysates were subjected to 24-hour incubation with RIP buffer containing magnetic protein A/G beads, which were coated with the antibodies specific to AGO2 (1:50; Abcam) and IgG (1:100; Abcam) as per the guidebook. The expressions of circ_0051079, miR-625-5p and TRIM66 in the sediments were detected by qRT-PCR.

2.12. Mouse xenograft model assay

Five-week-old male BALB/c nude mice were gained from Charles River (Beijing, China). Saos-2 cells infected with lentiviruse expressing sh-circ_0051079 or sh-NC were adjusted to 5×10^6 cells per 200 μL PBS. Then, the cells were subcutaneously injected into the back of mice. At the seventh day after injection, the volume of visible tumors was measured every 1 week for 4 cycles. The forming neoplasms were harvested and stored at −80 °C for further analysis of tumor weight and gene expression. The Animal Care and Use Committee of The Fifth people's Hospital of Dalian approved the study.

2.13. Statistical analysis

GraphPad Prism, image J software and Cell Quest software were employed to analyze the data from three independent duplicate tests. Results were expressed as means ± standard deviations. The significant differences were compared using Wilcoxon rank-sum test, Student's *t*-tests or analysis of variance. Chi-square test was used for comparing groups between high and low circ_0051079 expression. P value < 0.05 was considered statistically significant.

3. Results

3.1. Circ_0051079 expression was upregulated in OS tissues and cells

The expression of circ_0051079 was first analyzed in OS tissues. As shown in Fig. 1A, circ_0051079 expression was significantly upregulated in OS tissues in comparison with the neighboring non-tumor tissues. Meanwhile, we found that circ_0051079 expression was significantly associated with the TNM stage and tumor size of OS patients (Table 2). Also, circ_0051079 expression was higher in stage III OS tissues and the OS tissues sized > 5 cm than in stage I-II OS tissues or those < 5 cm (Fig. 1B and C). The data from Fig. 1D also showed that circ_0051079 was overexpressed in OS cell lines (U2OS, HOS and SaoS2) compared with normal osteoblast cell line (hFOB1.19). U2OS and SaoS2 cell lines were employed for the subsequent study owing to the higher expression of circ_0051079 in the two types of cell lines. Subsequently, there was no significant difference in circ_0051079 expression after RNase R treatment in U2OS and SaoS2 cells, although linear AKT2 expression was significantly reduced (Fig. 1E and F). These data demonstrated that circ_0051079 was upregulated in OS tissues and cells.

3.2. Circ_0051079 knockdown inhibited HUVEC angiogenesis and OS cell malignancy

To investigate the function of circ_0051079 in OS progression, we transfected siRNAs specific to circ_0051079 into both U2OS and SaoS2 cells to explore its effects on cell proliferation, migration, invasion, angiogenesis and apoptosis. The efficiency of circ_0051079 knockdown in U2OS and SaoS2 cells was shown in Fig. 2A and Fig. S1. si-circ_0051079#1 was chosen for the following study as its the highest knockdown efficiency. Then, we found that circ_0051079 silencing led to decreases in OD values and the number of positive colonies in both U2OS and SaoS2 cells (Fig. 2B-D), suggesting that circ_0051079

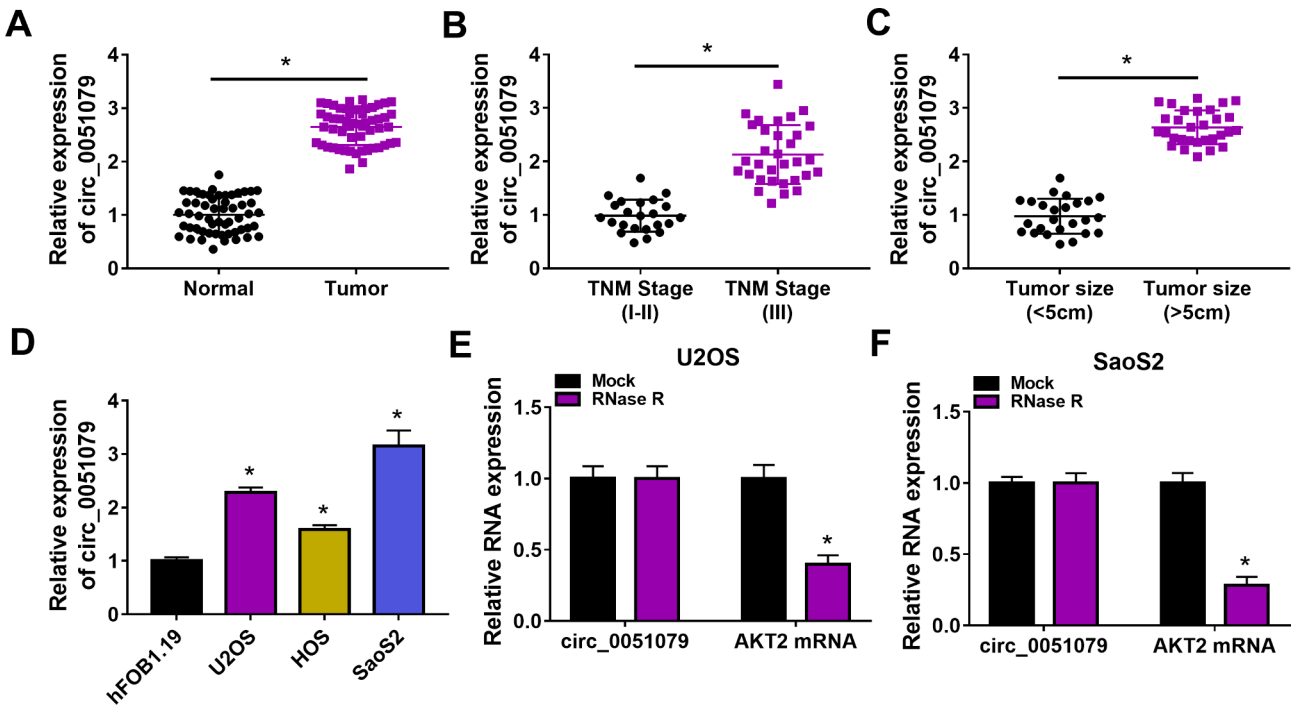

Fig. 1. The expression of circ_0051079 in OS tissues and cells. (A) Circ_0051079 expression was detected by qRT-PCR in OS tissues (N = 55) and adjacent non-tumor tissues (N = 55). (B and C) Circ_0051079 expression was checked by qRT-PCR in stage I-II OS tissues(N = 23), stage III OS tissues (N = 32), OS tissues sized < 5 cm (N = 25) and OS tissues sized > 5 cm (N = 30). (D) Circ_0051079 expression was determined by qRT-PCR in hFOB1.19, U2OS, HOS and SaoS2 cells. (E and F) The stability of circ_0051079 was identified by RNase R treatment assay. *$P < 0.05$.

Table 2
Relationship between clinical variables of OS patients and circ_0051079 level.

Variables	Cases (n)	Circ_0051709 expression (n)		*P*
		High (28)	Low (27)	
Age (years)				0.8984
≤25	29	15	14	
>25	26	13	13	
Gender				0.0804
Male	29	18	11	
Female	26	10	16	
Lung metastasis				0.1354
Present	26	16	10	
Absent	29	12	17	
TNM stage				0.0425*
I-II	23	8	15	
III	32	20	12	
Tumor size (cm)				0.0019*
≤5	25	7	18	
>5	30	21	9	

TNM tumor-node-metastasis; *$P < 0.05$, statistically significant.

depletion inhibited U2OS and SaoS2 cell proliferation. The migration and invasion of both U2OS and SaoS2 cells were also inhibited after circ_0051079 knockdown (Fig. 2E and F). Consistently, the tube formation of HUVECs was repressed by reducing circ_0051079 expression (Fig. 2G). On the contrary, decreasing circ_0051079 expression induced U2OS and SaoS2 cell apoptosis (Fig. 2H). PCNA and Bcl-2 expressions were decreased, but Bax expression was increased in circ_0051079-depleted U2OS and SaoS2 cells compared with controls (Fig. 2I and J). Further, the study analyzed the effects of circ_0051079 depletion on SaoS2 cell processes using shRNA of circ_0051079. The success of circ_0051079 knockdown in SaoS2 cells was shown in Fig. S2A. Meanwhile, circ_0051079 absence inhibited SaoS2 cell proliferation, migration, invasion and tube formation and induced cell apoptosis, accompanied by the decreases of PCNA and Bcl-2 expression and an increase of Bax (Fig. S2B-H). Thus, these findings demonstrated that circ_0051079 depletion repressed OS cell tumor properties.

3.3. *Circ_0051079 regulated TRIM66 expression by interacting with miR-625-5p in U2OS and SaoS2 cells*

To investigate the mechanism underlying circ_0051079 regulating OS cell processes, we performed circular RNA interactome and targetscan online databases to predict the target miRNA and mRNA of the circRNA. As shown in Fig. 3A, circ_0051079 contained the binding sites of miR-625-5p. To validate the interaction of circ_0051079 and miR-625-5p, qRT-PCR was used to determine the efficiency of miR-625-5p overexpression in U2OS and SaoS2 cells (Fig. 3B). Then, miR-625-5p overexpression dramatically inhibited the luciferase activity of wild-type reporter plasmid of circ_0051079 in U2OS and SaoS2 cells, but not the luciferase activity of mutant reporter plasmid of circ_0051079 (Fig. 3C and D). Meanwhile, the antibody specific to AGO2 significantly enriched both circ_0051079 and miR-625-5p in U2OS and SaoS2 cells (Fig. 3E and F). Comparatively, miR-625-5p expression was reduced in OS tissues and cells (U2OS, HOS and SaoS2) (Fig. 3G and H). The above data demonstrated that circ_0051079 combined with miR-625-5p in U2OS and SaoS2 cells.

As presented in Fig. 3I, miR-625-5p carried the possible binding sites of TRIM66. Dual-luciferase reporter assay also showed that miR-625-5p overexpression significantly reduced the luciferase activity of WT-TRIM66 3′UTR, but there was no significant difference in the luciferase activity of MUT-TRIM66 3′UTR (Fig. 3J and K). Also, both miR-625-5p and TRIM66 were significantly enriched in the anti-AGO2 group compared with the anti-IgG group (Fig. 3L and M). Consistently, TRIM66 was significantly increased in OS tissues and cells (U2OS, HOS and SaoS2) compared with the neighboring non-tumor tissues and normal osteoblast cell line (hFOB1.19) (Fig. 3N-P). Based on the above evidence, TRIM66 was employed as a target mRNA of miR-625-5p. Given the interplay between miR-625-5p and circ_0051079 or TRIM66, the study further explored whether circ_0051079 mediated TRIM66 expression by miR-625-5p. As expected, the mRNA and protein

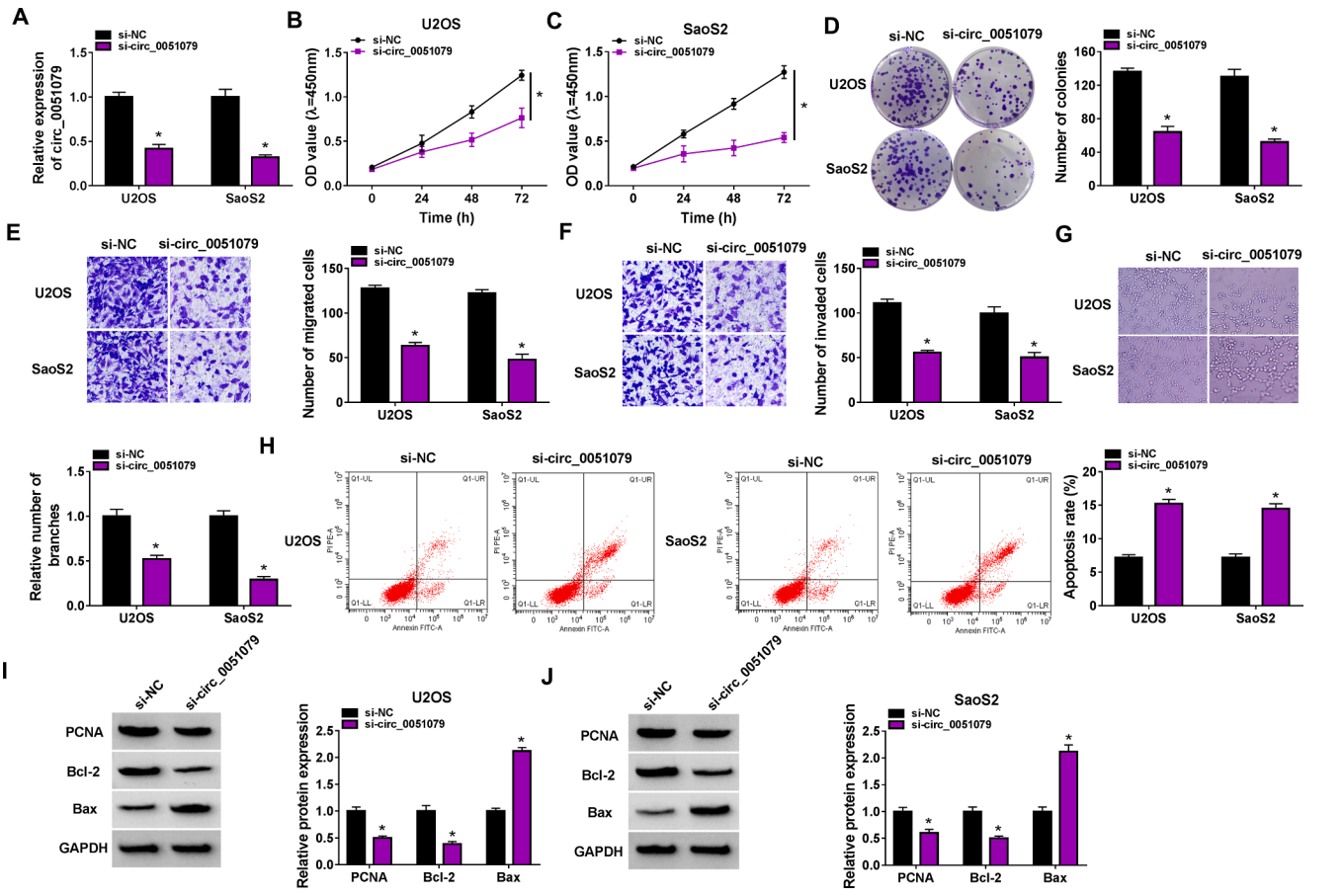

Fig. 2. The effects of circ_0051079 knockdown on OS cell processes. (A-J) Both U2OS and SaoS2 cells were transfected with si-NC or si-circ_0051079, and the efficiency of si-circ_0051079 transfection was determined by qRT-PCR (A), cell proliferation by CCK-8 and clonogenicity assays (B-D), migration and invasion by transwell assays (E and F), angiogenesis by tube formation assay (G), cell apoptosis by flow cytometry analysis (H), and the protein expressions of PCNA, Bcl-2 and Bax by Western blot analysis (I and J). $^*P < 0.05$.

expressions of TRIM66 were reduced after circ_0051079 knockdown, which was reversed by decreasing miR-625-5p expression (Fig. 3Q and R). Thus, circ_0051079 mediated TRIM66 expression through miR-625-5p.

3.4. MiR-625-5p depletion partially attenuated circ_0051079 knockdown-induced effects in U2OS and SaoS2 cells

Given the binding relationship of circ_0051079 and miR-625-5p, the study continued to investigate whether miR-625-5p participated in circ_0051079-mediated OS cell processes. qRT-PCR was carried out to detect the efficiency of miR-625-5p knockdown in U2OS and SaoS2 cells (Fig. 4A). Subsequently, circ_0051079 knockdown increased miR-625-5p expression in U2OS and SaoS2 cells, whereas the effect was partially relieved after miR-625-5p silencing (Fig. 4B). The inhibitory effects of circ_0051079 knockdown on the proliferation, migration and invasion of U2OS and SaoS2 cells were partially restored after down-regulation of miR-625-5p (Fig. 4C-G). Consistently, the weakened angiogenetic ability of HUVECs by circ_0051079 depletion was partially remitted after transfection with miR-625-5p inhibitors (Fig. 4H). MiR-625-5p quietness also partially counteracted circ_0051079 depletion-induced apoptosis of U2OS and SaoS2 cells (Fig. 4I). It was discovered using Western blot analysis that the reduced expression of PCNA and Bcl-2 and increased expression of Bax by circ_0051079 exhaustion were partially rescued after miR-625-5p downregulation in U2OS and SaoS2 cells (Fig. 4J and K). Collectively, these data demonstrated that circ_0051079 regulated OS cell malignancy and angiogenesis by interacting with miR-625-5p.

3.5. Circ_0051079 regulated the malignant phenotypes of OS cells by interacting with miR-625-5p/TRIM66 pathway

Considering the interplay of miR-625-5p with circ_0051079 and TRIM66, we further analyzed whether the regulation of circ_0051079 in OS cell malignancy involved the miR-625-5p/TRIM66 pathway. Firstly, the overexpression plasmid of TRIM66 was transfected into both U2OS and SaoS2 cells, and Western blot analysis was conducted to determine the efficiency of TRIM66 overexpression. As displayed in Fig. 5A, TRIM66 expression was significantly increased in both the U2OS and SaoS2 cells transfected with the overexpression plasmid of TRIM66 compared with the cells transfected with vector, showing the high efficiency of TRIM66 overexpression. Then, we found that miR-625-5p introduction decreased TRIM66 production in U2OS and SaoS2 cells, which was partially attenuated by the increased expression of TRIM66 (Fig. 5B). The inhibitory effects of miR-625-5p overexpression on U2OS and SaoS2 cell proliferation, migration and invasion were partially attenuated after transfection with TRIM66 (Fig. 5C-G). Consistently, the weakened angiogenetic ability of HUVEC and increased U2OS and SaoS2 cell apoptosis rate by miR-625-5p were partially remitted after TRIM66 overexpression (Fig. 5H and I). Comparatively, miR-625-5p introduction resulted in decreases of PCNA and Bcl-2 production and an increase of Bax production in U2OS and SaoS2 cells; however, these effects were partially remitted by ectopic expression of TRIM66 (Fig. 5J and K). Further, we analyzed the effects of circ_0051079 depletion and TRIM66 overexpression on U2OS and SaoS2 cell processes. As shown in Fig. S3A, circ_0051079 knockdown decreased TRIM66 expression in U2OS and SaoS2 cells, whereas the effect was relieved by increasing

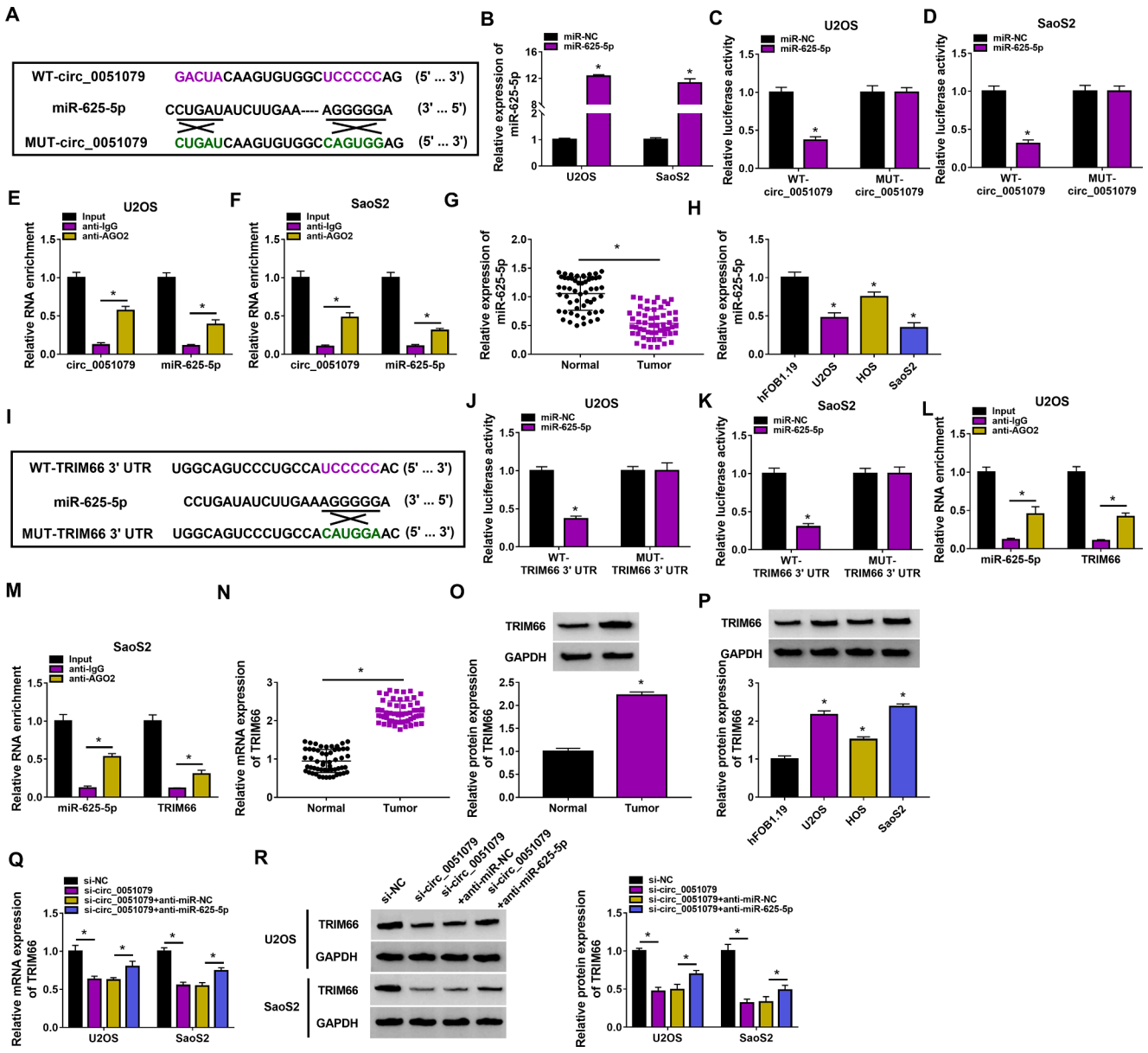

Fig. 3. Circ_0051079 mediated TRIM66 expression by inhibiting miR-625-5p. (A and I) The schematic illustration showing the complementary sites of miR-625-5p with circ_0051079 and TRIM66. (B) The efficiency of miR-625-5p overexpression was detected by qRT-PCR. (C, D, J and K) Dual-luciferase reporter assay was employed to determine the association of miR-625-5p with circ_0051079 or TRIM66. (E, F, L and M) RIP assay was used to identify the interplay of miR-625-5p and circ_0051079 or TRIM66. (G and H) MiR-625-5p expression was detected by qRT-PCR in OS tissues (N = 55), adjacent non-tumor tissues (N = 55), hFOB1.19 cells, U2OS cells, HOS cells and SaoS2 cells. (N-P) TRIM66 expression was checked by qRT-PCR and Western blot analysis in OS tissues, adjacent non-tumor tissues, hFOB1.19 cells, U2OS cells, HOS cells and SaoS2 cells. (Q and R) The effects between circ_0051079 knockdown and miR-625-5p downregulation on TRIM66 expression were determined by qRT-PCR and Western blot analysis. $^*P < 0.05$.

TRIM66 expression. Meanwhile, we found that circ_0051079 absence repressed U2OS and SaoS2 cell proliferation, migration and invasion and HUVEC tube formation and induced U2OS and SaoS2 cell apoptosis, accompanied by the decreases of PCNA and Bcl-2 expression and an increase of Bax; however, these effects were attenuated when TRIM66 expression was increased (Fig. S3B-K). Taken together, all findings suggested that circ_0051079 regulated the malignant phenotypes of OS cells by interacting with miR-625-5p and TRIM66.

3.6. Circ_0051079 regulated Wnt/β-catenin pathway by TRIM66

At present, more studies have shed light on the role of the Wnt/β-catenin pathway in cancer development. Herein, we analyzed the effects between circ_0051079 and TRIM66 on the Wnt/β-catenin pathway in U2OS and SaoS2 cells. To clarify this, we silenced circ_0051079 and overexpressed TRIM66 in both U2OS and SaoS2 cells. As shown in Fig. 6A and B, the production of Wnt/β-catenin pathway signal proteins, β-catenin, c-myc and cyclinD1, was inhibited after circ_0051079 knockdown in U2OS and SaoS2 cells; however, TRIM66 introduction extenuated the effects caused by circ_0051079, suggesting that circ_0051079 could regulate Wnt/β-catenin pathway through TRIM66.

3.7. Circ_0051079 knockdown inhibited tumor formation in vivo

Saos-2 cells transfected with sh-circ_0051079 or sh-NC were injected into nude mice to further investigate the anti-cancer effects of circ_0051079 silencing *in vivo*. After 28 days, the volume and weight of primary tumors from Saos-2 cells were smaller in the sh-circ_0051079

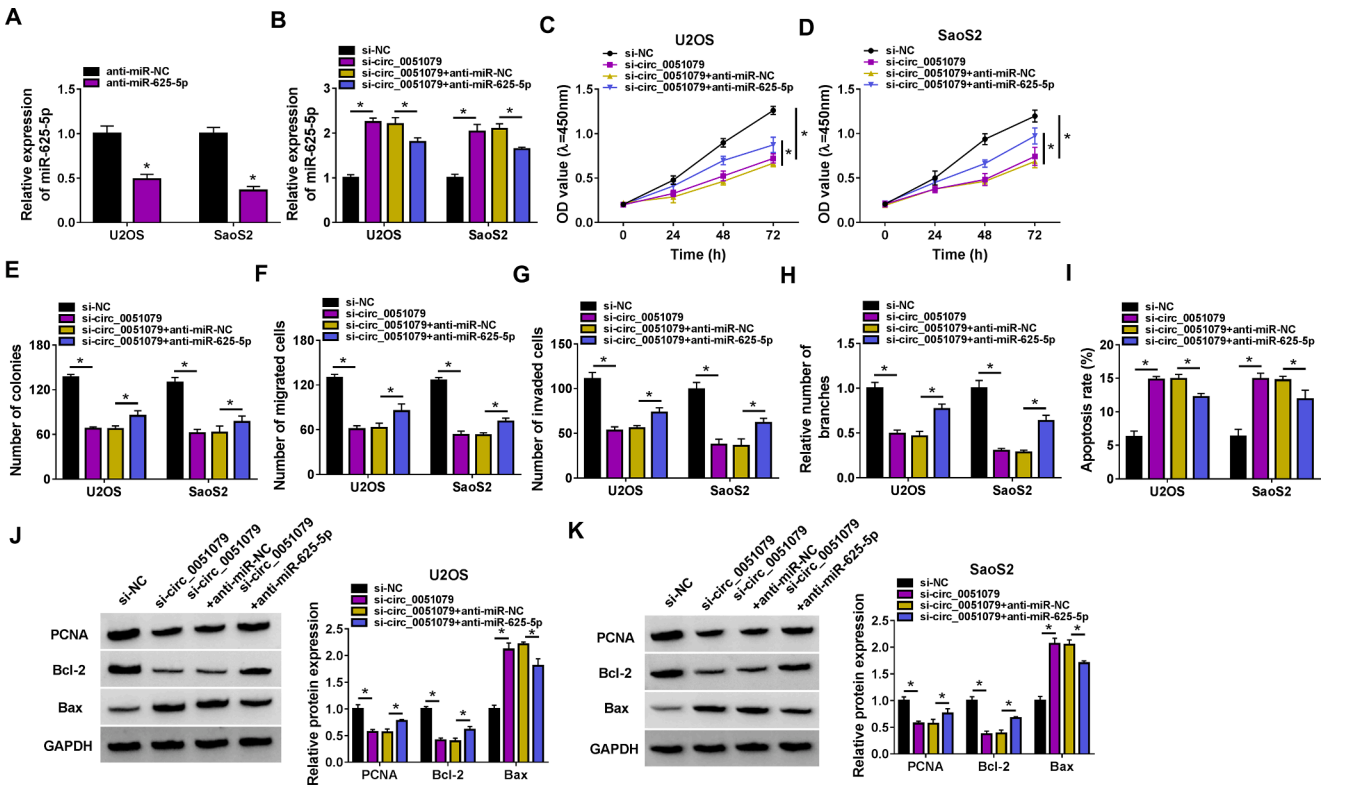

Fig. 4. The effects between circ_0051079 knockdown and miR-625-5p depletion on U2OS and SaoS2 cell processes. (A) The efficiency of anti-miR-625-5p in reducing miR-625-5p expression was detected by qRT-PCR. (B-K) U2OS and SaoS2 cells were transfected with si-NC, si-circ_0051079, si-circ_0051079 + anti-miR-NC or si-circ_0051079 + anti-miR-625-5p, and miR-625-5p expression was determined by qRT-PCR (B), cell proliferation by CCK-8 and clonogenicity assays (C-E), migration and invasion by transwell assays (F and G), angiogenesis by tube formation assay (H), cell apoptosis by flow cytometry analysis (I), and the protein expression of PCNA, Bcl-2 and Bax by Western blot analysis (J and K). *$P < 0.05$.

groups than in the sh-NC groups (Fig. 7A-C). Then, the study confirmed that circ_0051079 knockdown reduced the expressions of circ_0051079 and TRIM66 but increased miR-625-5p expression in the forming tumors (Fig. 7D and E). MiR-625-5p was negatively correlated with circ_0051079 and TRIM66, and circ_0051079 was positively correlated with TRIM66 in the primary tumors from Saos-2 cells (Fig. 7F-H). Further, the expression of metastasis-related MMP2 and MMP9 was repressed in the primary tumors from the sh-circ_0051079 group when compared with the primary tumors from the sh-NC group (Fig. 7I). In conclusion, circ_0051079 silencing inhibited the malignant progression of Saos-2 cells by regulating miR-625-5p and TRIM66 *in vivo*.

4. Discussion

OS arises from bone-forming mesenchymal cells and mainly damages the metaphyseal region of the long bones. At present, the lung-targeted metastasis induced by OS is considered as the major reason for poor prognosis. Convincing evidence has indicated that circRNA serves key parts in OS and has the potential as a therapeutic target for different diseases. For example, circRNA endothelin converting enzyme 1 (circECE1) silencing suppressed OS cell proliferation and tumor metastasis by promoting glucose metabolism through associating with c-myc [25]. Knockdown of circRNA myosin X inhibited endothelial-mesenchymal transition by regulating β-catenin/lymphoid enhancer factor-1 (LEF1) complex in a miR-370-3p-dependent manner [26]. Circ_103801 might mediate OS progression through several signaling pathways like the angiogenesis pathway and the PI3K-Akt signaling pathway [27]. In the present study, we reported the abnormal expression of circ_0051079 in OS, and demonstrated that circ_0051079 might contribute to OS progression by regulating the miR-625-5p/TRIM66 axis.

AKT family is well known for modulating cancer development and progression [28]. As a member of the AKT family, AKT2 is widely distributed in human tissues. Compared with other AKT members like AKT1 and AKT3, AKT2 is more closely associated with proliferation, metastasis and angiogenesis of cancer cells [29]. In particular, previous data have suggested that AKT2 contributes to OS cell proliferation and migration through binding to miR-200c [30]. Circ_0051079, located in chr19:40747844-40771258, is formed by cyclization of exons 2–6 of AKT2 gene; however, little is known about the mechanism of the circRNA in mediating OS progression. In the present study, we found the high expression of circ_0051079 in OS tissues compared with controls, especially in stage III OS tissues and these tissues sized > 5 cm. Circ_0051079 expression was significantly associated with the TNM stage and tumor size of OS patients. Meanwhile, circ_0051079 was augmented in OS cell lines. The study also demonstrated that circ_0051079 silencing led to repression of cell proliferation, cell metastasis and tumor formation, which was approved by a previous report [12]. Besides, we reported for the first time that circ_0051079 promoted angiogenesis and inhibited OS cell apoptosis.

MiRNA has been confirmed to be widely expressed in cancer tissues, highlighting its critical roles in tumor onset and development. As a miRNA, miR-625-5p is important for cancer progression. A recent study reported that miR-625-5p participated in the regulation of glioma cell migration and invasion by binding to circ_0002142 [18]. Shang and his colleagues indicated that miR-625-5p regulated CRC cell proliferation and invasion by combining with LIM and SH3 protein 1 (LASP1) [31]. Another study expounded that miR-625-5p predicted better survival in cervical cancer and its introduction repressed cell growth by modulating nuclear factor kappa B signaling [32]. In particular, miR-625-5p has been found to inhibit OS cell proliferation and invasion by reducing the expression of Yes-associated protein 1 (YAP-1) [33]. Herein, miR-625-5p was identified as a target miRNA of circ_0051079. Comparative

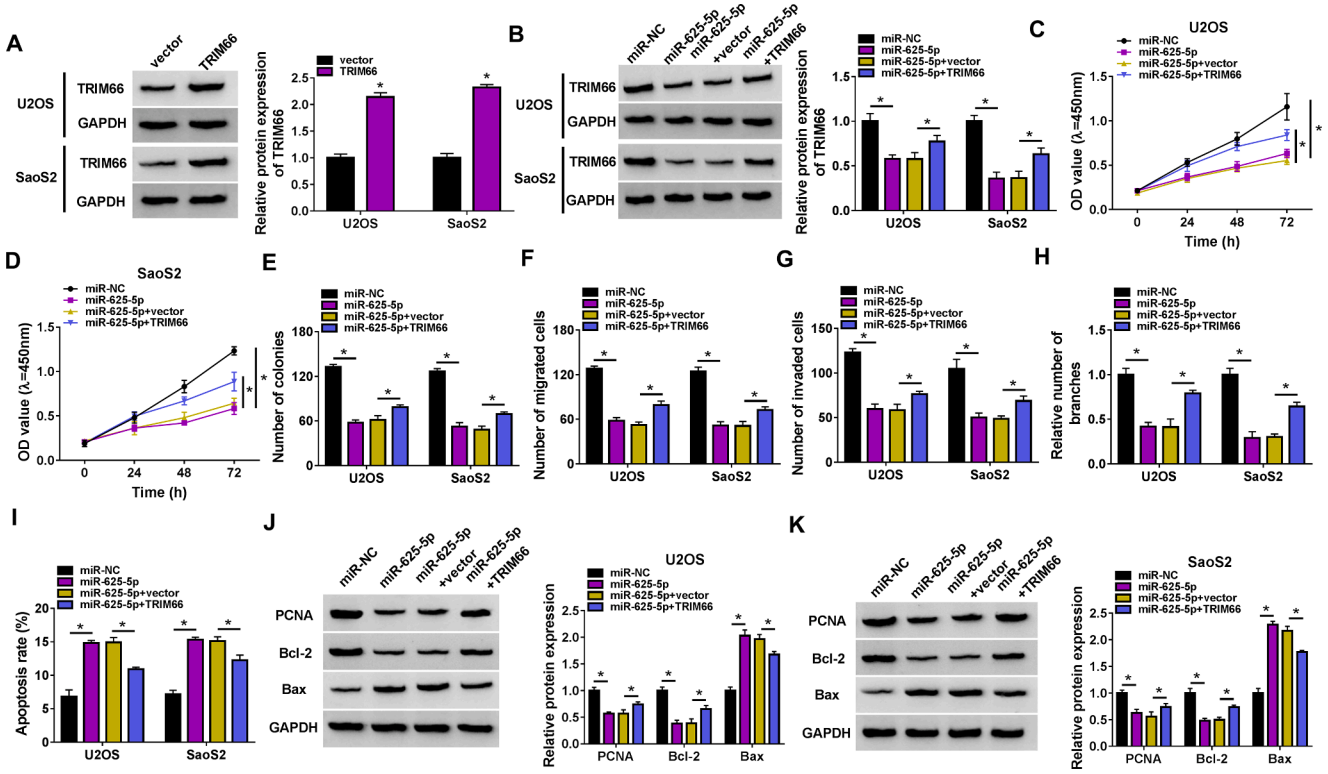

Fig. 5. The effects between miR-625-5p and TRIM66 on OS cell processes. (A) The efficiency of TRIM66 overexpression was detected by Western blot analysis. (B-K) U2OS and SaoS2 cells were transfected with miR-NC, miR-625-5p, miR-625-5p + vector or miR-625-5p + TRIM66, and TRIM66 protein expression was analyzed by Western blot (B), cell proliferation by CCK-8 and clonogenicity assays (C-E), migration and invasion by transwell assays (F and G), angiogenesis by tube formation assay (H), cell apoptosis by flow cytometry analysis (I), and the protein expressions of PCNA, Bcl-2 and Bax by Western blot analysis (J and K). $^*P < 0.05$.

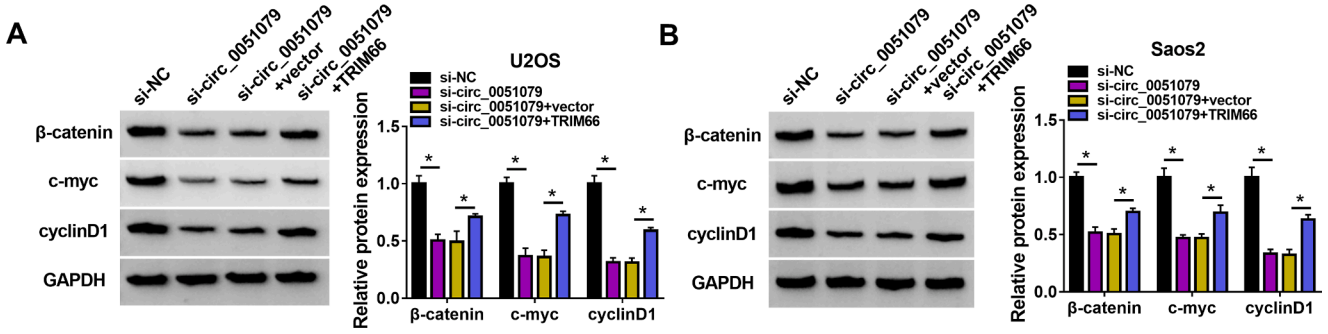

Fig. 6. Circ_0051079 regulated Wnt/β-catenin pathway through TRIM66. (A and B) The effects between circ_0051079 knockdown and TRIM66 overexpression on the production of β-catenin, c-myc and cyclinD1 were determined by Western blot analysis. $^*P < 0.05$.

analysis showed that miR-625-5p was downregulated in OS tissues and cells. Importantly, circ_0051079 regulated OS cell malignancy by binding to miR-625-5p.

Several investigations indicated that TRIM66 acted as an oncogene in various cancers. Cao *et al.* explained that TRIM66 knockdown weakened the migratory and invasive capacities of prostate cancer cells by the JAK/STAT pathway [34]. Zhang and his colleagues testified that TRIM66 deficiency inhibited hepatocellular carcinoma cell proliferation but promoted cell apoptosis through the epithelial-mesenchymal transition pathway [21]. In the work of Dai *et al.*, we found that TRIM66 silencing inhibited lung cancer cell proliferation and motility [35]. Herein, the binding relationship between TRIM66 and miR-625-5p was confirmed by mechanism assays. The data from qRT-PCR and Western blot exhibited that TRIM66 was elevated in OS tissues and cells. Consistent with a previous study [36], the results from the functional analysis showed that TRIM66 promoted OS cell proliferation and motility but inhibited cell apoptosis. In addition, increasing expression of TRIM66 contributed to angiogenesis. Moreover, TRIM66 was implicated in miR-625-5p and circ_0051079-mediated OS malignant progression. Very importantly, we provided evidence that circ_0051079 regulated TRIM66 expression by miR-625-5p.

Wnt/β-catenin signaling is one of the Wnt signaling pathways that play important parts in regulating tissue homeostasis, including the skeletal system, and its activation acts as a genetic driver in multiple cancers [37]. The accumulation of unphosphorylated β-catenin turns on Wnt target proteins like c-myc and cyclinD1 through specific factors and co-activators, such as Pygopus (Pygo) and Bcl-9 [38]. Considerable evidence has proved that OS progression involves the activation of the signaling pathway [39]. As reported by Li *et al.*, some factors, such as hormones and alkaline phosphatase, mediated the participation of Wnt/β-catenin signaling in OS progression [40]. In particular, it has been revealed that TRIM66 contributes to cancer development by the Wnt/

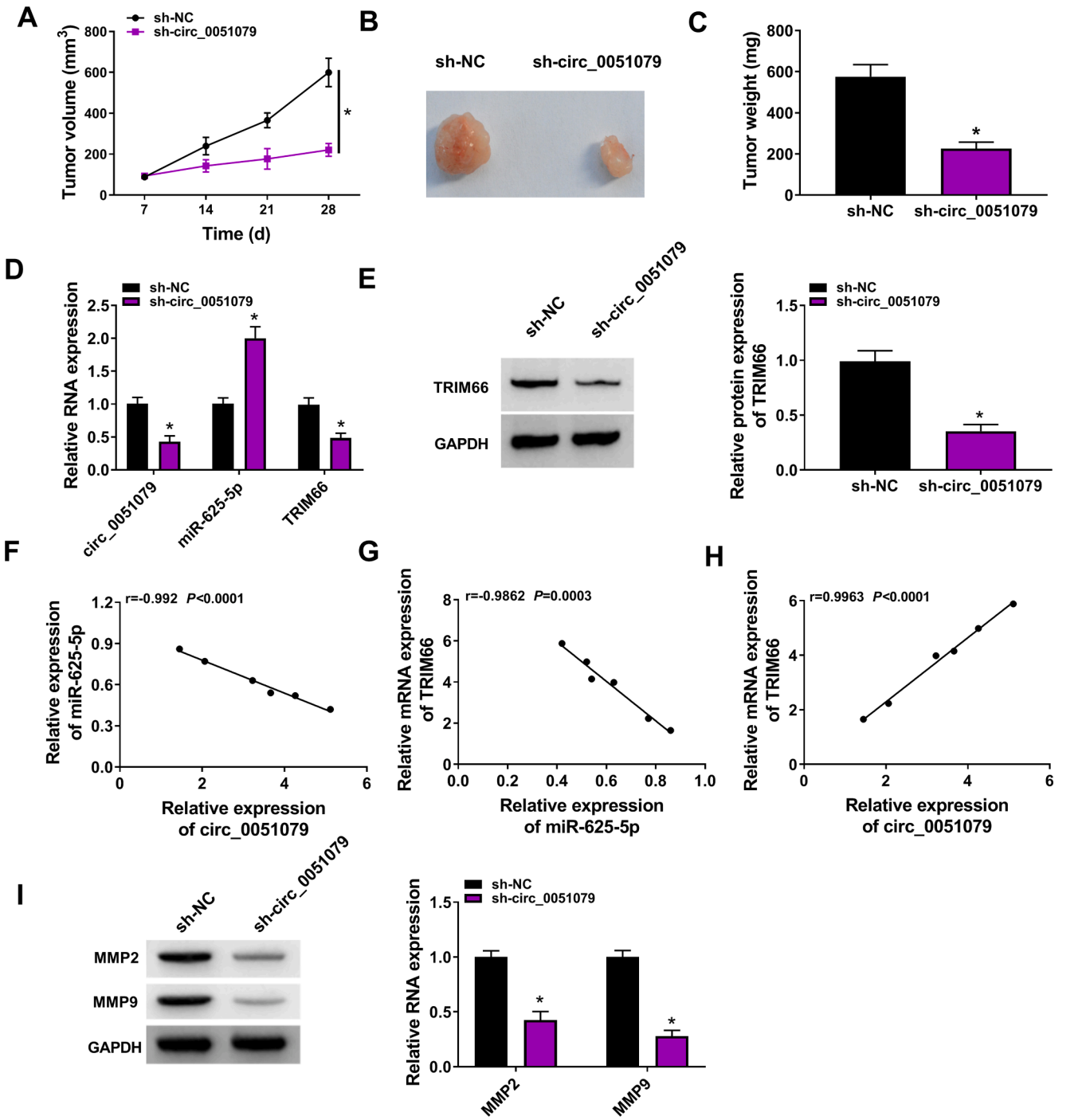

Fig. 7. The effects of circ_0051079 on the malignant progression of OS cells *in vivo*. (A-C) The impacts of circ_0051079 knockdown on the volume and weight of forming tumors. (D and E) The effects of circ_0051079 depletion on the expressions of circ_0051079, miR-625-5p and TRIM66 were analyzed by qRT-PCR and Western blot in the primary tumors from Saos-2 cells. (F-H) The correlations among circ_0051079, miR-625-5p and TRIM66 were analyzed by Spearman correlation analysis in the primary tumor tissues from Saos-2 cells. (I) Western blot was performed to detect MMP2 and MMP9 expression in the primary tumors from Saos-2 cells. $^*P < 0.05$.

β-catenin signaling [41]. In this work, we found that circ_0051079 depletion reduced the expression of β-catenin, c-myc and cyclinD1, which was attenuated by ectopic expression of TRIM66, suggesting that TRIM66/Wnt/β-catenin signaling pathway might be required for the regulation of circ_0051079 in OS cell malignancy.

Nevertheless, the major shortcoming of the study was that there was no data about the association between TRIM66 and Wnt/β-catenin signaling in OS cells. Although our results have explained that TRIM66 can regulate Wnt target proteins, the underlying mechanism needs to be investigated in further research. In addition, we analyzed the effect of circ_0051079 on tumor formation *in vivo* by subcutaneously injecting SaOS2 cells into nude mice. Given that the bone microenvironment plays an important role in the pathophysiology of OS, the *in vivo* assay should be further performed using a mouse model with para-tibial injection of OS cells.

Taken together, OS malignant progression might be associated with circ_0051079 overexpression. The mechanism regarding the function of circ_0051079 in OS progression was partly attributed to the

circ_0051079/miR-625-5p/TRIM66/Wnt/β-catenin signaling. The novel finding suggested the potential of circ_0051079 as a target for osteosarcoma intervention.

Ethics approval and consent to participate

The present study was approved by the ethical review committee of the Fifth people's Hospital of Dalian. Written informed consent was obtained from all enrolled patients.

Consent for publication

Patients agree to participate in this work.

Availability of data and materials

The analyzed data sets generated during the present study are available from the corresponding author on reasonable request.

CRediT authorship contribution statement

Weilin Wang: Validation, Investigation, Writing – original draft, Writing – review & editing. **Jianhua Wang:** Conceptualization, Methodology, Validation, Investigation, Writing – original draft, Writing – review & editing, Project administration. **Yingyi Li:** Conceptualization, Methodology, Formal analysis, Data curation, Writing – original draft, Writing – review & editing. **Yongxu Zhao:** Formal analysis, Data curation, Software.

Declaration of Competing Interest

The authors declare that they have no known competing financial interests or personal relationships that could have appeared to influence the work reported in this paper.

Acknowledgement

None.

Funding

No funding was received.

Disclosure of interest

The authors declare that they have no financial or non-financial conflicts of interest.

Appendix A. Supplementary data

Supplementary data to this article can be found online at https://doi.org/10.1016/j.jbo.2022.100436.

References

[1] Ritter J, Bielack SS. Osteosarcoma. Ann Oncol. 2010;21 Suppl 7:vii320-325.
[2] M. Sampo, M. Koivikko, M. Taskinen, P. Kallio, A. Kivioja, M. Tarkkanen, T. Böhling, Incidence, epidemiology and treatment results of osteosarcoma in Finland - a nationwide population-based study, Acta Oncol. (Stockholm, Sweden). 50 (8) (2011) 1206–1214.
[3] B. Otoukesh, B. Boddouhi, M. Moghtadaei, P. Kaghazian, M. Kaghazian, Novel molecular insights and new therapeutic strategies in osteosarcoma, Cancer Cell Int. 18 (2018) 158.
[4] M.W. Bishop, K.A. Janeway, R. Gorlick, Future directions in the treatment of osteosarcoma, Curr. Opin. Pediatr. 28 (2016) 26–33.
[5] G. Lu, J. Zhang, X. Liu, W. Liu, G. Cao, C. Lv, X. Zhang, P. Xu, M. Li, X. Song, Regulatory network of two circRNAs and an miRNA with their targeted genes under astilbin treatment in pulmonary fibrosis, J. Cell Mol. Med. 23 (2019) 6720–6729.
[6] S. Memczak, P. Papavasileiou, O. Peters, N. Rajewsky, S. Pfeffer, Identification and characterization of circular RNAs as a new class of putative biomarkers in human blood, PLoS ONE 10 (2015) e0141214.
[7] Y. Yao, X. Chen, H. Yang, W. Chen, Y. Qian, Z. Yan, T. Liao, W. Yao, W. Wu, T. Yu, Y. Chen, Y. Zhang, Hsa_circ_0058124 promotes papillary thyroid cancer tumorigenesis and invasiveness through the NOTCH3/GATAD2A axis, J. Exp. Clin. Cancer Res. 38 (2019) 318.
[8] X. Li, S. Lin, Z. Mo, J. Jiang, H. Tang, C. Wu, J. Song, CircRNA_100395 inhibits cell proliferation and metastasis in ovarian cancer via regulating miR-1228/p53/epithelial-mesenchymal transition (EMT) axis, J. Cancer 11 (2020) 599–609.
[9] Y. Ma, X. Cong, Y. Zhang, X. Yin, Z. Zhu, Y. Xue, CircPIP5K1A facilitates gastric cancer progression via miR-376c-3p/ZNF146 axis, Cancer Cell Int. 20 (2020) 81.
[10] L.S. Kristensen, M.S. Andersen, L.V.W. Stagsted, K.K. Ebbesen, T.B. Hansen, J. Kjems, The biogenesis, biology and characterization of circular RNAs, Nat. Rev. Genet. 20 (2019) 675–691.
[11] Z. Li, X. Li, D. Xu, X. Chen, S. Li, L. Zhang, M.T.V. Chan, W.K.K. Wu, An update on the roles of circular RNAs in osteosarcoma, Cell Prolif. 54 (2021) e12936.
[12] Zhang Z, Zhao M, Wang G. Hsa_circ_0051079 functions as an oncogene by regulating miR-26a-5p/TGF-β1 in osteosarcoma. Cell Biosci. 2019;9:94.
[13] Y. Lv, C. Lu, X. Ji, Z. Miao, W. Long, H. Ding, M. Lv, Roles of microRNAs in preeclampsia, J. Cell. Physiol. 234 (2019) 1052–1061.
[14] Z. Ali Syeda, S.S.S. Langden, C. Munkhzul, M. Lee, S.J. Song, Regulatory mechanism of MicroRNA expression in cancer, Int. J. Mol. Sci. 21 (2020) 1723.
[15] J. Zhang, Y.G. Yan, C. Wang, S.J. Zhang, X.H. Yu, W.J. Wang, MicroRNAs in osteosarcoma, Clin. Chim. Acta 444 (2015) 9–17.
[16] R. Dao, M. Wudu, L. Hui, J. Jiang, Y. Xu, H. Ren, X. Qiu, Knockdown of lncRNA MIR503HG suppresses proliferation and promotes apoptosis of non-small cell lung cancer cells by regulating miR-489-3p and miR-625-5p, Pathol. Res. Pract. 216 (2020) 152823.
[17] L. Wang, Y. Zhong, B. Yang, Y. Zhu, X. Zhu, Z. Xia, J. Xu, L. Xu, LINC00958 facilitates cervical cancer cell proliferation and metastasis by sponging miR-625-5p to upregulate LRRC8E expression, J. Cell. Biochem. 121 (2020) 2500–2509.
[18] H. Su, D. Zou, Y. Sun, Y. Dai, Hypoxia-associated circDENND2A promotes glioma aggressiveness by sponging miR-625-5p, Cell. Mol. Biol. Lett. 24 (2019) 24.
[19] S. Hatakeyama, TRIM proteins and cancer, Nat. Rev. Cancer 11 (2011) 792–804.
[20] K. Khetchoumian, M. Teletin, M. Mark, T. Lerouge, M. Cerviño, M. Oulad-Abdelghani, et al., TIF1delta, a novel HP1-interacting member of the transcriptional intermediary factor 1 (TIF1) family expressed by elongating spermatids, J. Biol. Chem. 279 (2004) 48329–48341.
[21] H.G. Zhang, Y.W. Pan, J. Feng, C.T. Zeng, X.Q. Zhao, B. Liang, et al., TRIM66 promotes malignant progression of hepatocellular carcinoma by inhibiting E-cadherin expression through the EMT pathway, Eur. Rev. Med. Pharmacol. Sci. 23 (2019) 2003–2012.
[22] X. Qi, D.-H. Zhang, N. Wu, J.-H. Xiao, X. Wang, W. Ma, ceRNA in cancer: possible functions and clinical implications, J. Med. Genet. 52 (2015) 710–718.
[23] Z. He, X. Ruan, X. Liu, J. Zheng, Y. Liu, L. Liu, J. Ma, L. Shao, D.i. Wang, S. Shen, C. Yang, Y. Xue, FUS/circ_002136/miR-138-5p/SOX13 feedback loop regulates angiogenesis in Glioma, J. Exp. Clin. Cancer Res. 38 (2019) 65.
[24] H. Xu, X. Sun, Y. Huang, Q. Si, M. Li, Long non-coding RNA NEAT1 modifies cell proliferation, colony formation, apoptosis, migration and invasion via the miR-4500/BZW1 axis in ovarian cancer, Mol. Med. Rep. 22 (2020) 3347–3357.
[25] S. Shen, T. Yao, Y. Xu, D. Zhang, S. Fan, J. Ma, CircECE1 activates energy metabolism in osteosarcoma by stabilizing c-Myc, Mol. Cancer 19 (2020) 151.
[26] J. Chen, G. Liu, Y. Wu, J. Ma, H. Wu, Z. Xie, S. Chen, Y. Yang, S. Wang, P. Shen, Y. Fang, S. Fan, S. Shen, X. Fang, CircMYO10 promotes osteosarcoma progression by regulating miR-370-3p/RUVBL1 axis to enhance the transcriptional activity of β-catenin/LEF1 complex via effects on chromatin remodeling, Mol Cancer. 18 (2019) 150.
[27] W. Liu, J. Zhang, C. Zou, X. Xie, Y. Wang, B.o. Wang, Z. Zhao, J. Tu, X. Wang, H. Li, J. Shen, J. Yin, Microarray expression profile and functional analysis of circular RNAs in osteosarcoma, Cell. Physiol. Biochem. 43 (2017) 969–985.
[28] I. Hers, E.E. Vincent, J.M. Tavaré, Akt signalling in health and disease, Cell. Signal. 23 (2011) 1515–1527.
[29] H. Li, S. Lu, Y. Chen, L. Zheng, L. Chen, H. Ding, J. Ding, D. Lou, F. Liu, B. Zheng, AKT2 phosphorylation of hexokinase 2 at T473 promotes tumorigenesis and metastasis in colon cancer cells via NF-κB, HIF1α, MMP2, and MMP9 upregulation, Cell. Signal. 58 (2019) 99–110.
[30] Y. Liu, S.-T. Zhu, X. Wang, J. Deng, W.-H. Li, P. Zhang, B.-S. Liu, MiR-200c regulates tumor growth and chemosensitivity to cisplatin in osteosarcoma by targeting AKT2, Sci. Rep. 7 (2017) 13598.
[31] T. Shang, X. Zhou, W. Chen, LINC01123 promotes progression of colorectal cancer via miR-625-5p/LASP1 axis, Cancer Biother. Radiopharm. (2020).
[32] Y. Li, Y. Ding, N. Ding, H. Zhang, M. Lu, X. Cui, X. Yu, MicroRNA-625-5p sponges lncRNA MALAT1 to Inhibit cervical carcinoma cell growth by suppressing NF-κB signaling, Cell Biochem. Biophys. 78 (2020) 217–225.
[33] Z. Luo, G. Wu, D. Zhang, J. Liu, R. Ran, microRNA-625 targets Yes-associated protein 1 to suppress cell proliferation and invasion of osteosarcoma, Mol. Med. Rep. 17 (2018) 2005–2011.
[34] H. Cao, R. Gao, L. Chen, Y. Feng, TRIM66 promotes malignant progression of prostate carcinoma through the JAK/STAT pathway, FEBS Open Bio. 10 (2020) 515–524.
[35] H.-y. Dai, Y. Ma, Z. Da, X.-M. Hou, Knockdown of TRIM66 inhibits malignant behavior and epithelial-mesenchymal transition in non-small cell lung cancer, Pathol. Res. Pract. 214 (2018) 1130–1135.

[36] Y.u. Chen, Y. Guo, H. Yang, G. Shi, G. Xu, J. Shi, N.a. Yin, D. Chen, TRIM66 overexpresssion contributes to osteosarcoma carcinogenesis and indicates poor survival outcome, Oncotarget 6 (2015) 23708–23719.
[37] N. Krishnamurthy, R. Kurzrock, Targeting the Wnt/beta-catenin pathway in cancer: update on effectors and inhibitors, Cancer Treat. Rev. 62 (2018) 50–60.
[38] M.D. Gordon, R. Nusse, Wnt signaling: multiple pathways, multiple receptors, and multiple transcription factors, J. Biol. Chem. 281 (2006) 22429–22433.
[39] F. Fang, A. VanCleave, R. Helmuth, H. Torres, K. Rickel, H. Wollenzien, H. Sun, E. Zeng, J. Zhao, J. Tao, Targeting the Wnt/β-catenin pathway in human osteosarcoma cells, Oncotarget 9 (2018) 36780–36792.
[40] C. Li, X. Shi, G. Zhou, X. Liu, S. Wu, J. Zhao, The canonical Wnt-beta-catenin pathway in development and chemotherapy of osteosarcoma, Front. Biosci. (Landmark Ed). 18 (2013) 1384–1391.
[41] W. Fan, F. Du, X. Liu, TRIM66 confers tumorigenicity of hepatocellular carcinoma cells by regulating GSK-3β-dependent Wnt/β-catenin signaling, Eur. J. Pharmacol. 850 (2019) 109–117.